

Thermal Conductivity of Anharmonic Lattices: Effective Phonons and Quantum Corrections

Dahai He^{1,*}, Sahin Buyukdagli^{1,†} and Bambi Hu^{1,2}

¹*Department of Physics, Centre for Nonlinear Studies,
and the Beijing- Hong Kong- Singapore Joint Centre
for Nonlinear and Complex Systems (Hong Kong),*

Hong Kong Baptist University, Kowloon Tong, Hong Kong, China

²*Department of Physics, University of Houston, Houston, Texas 77204-5005, USA*

(Dated: May 23, 2022)

Abstract

We compare two effective phonon theories, which have both been applied recently to study heat conduction in anharmonic lattices. In particular, we study the temperature dependence of the thermal conductivity of Fermi-Pasta-Ulam β model via the Debye formula, showing the equivalence of both approaches. The temperature for the minimum of the thermal conductivity and the corresponding scaling behavior are analytically calculated, which agree well with the result obtained from non-equilibrium simulations. We also give quantum corrections for the thermal conductivity from quantum self-consistent phonon theory. The vanishing behavior at low temperature regime and the existence of an *umklapp* peak are qualitatively consistent with experimental studies.

PACS numbers: 44.05.+e, 44.10.+i, 05.70.Ln, 63.20-e

*Electronic address: dhhe@hkbu.edu.hk

†Electronic address: sbuyukda@hkbu.edu.hk

The study of heat conduction is very important from both theoretical and experimental point of view. A traditional phenomenological approach to understand the thermal properties in solids is the Debye formula given by

$$\kappa = \sum_k C_k v_k l_k, \quad (1)$$

where κ is the thermal conductivity, C_k , v_k , l_k are the specific heat, the phonon group velocity and the phonon mean free path of mode k , respectively. In spite of its successfulness for qualitative explanation of heat conduction in dielectrics, quantitative predictions are hard to make from a microscopic viewpoint.

Recently, an increasing study of heat conduction in low dimensional Hamiltonian models may shed light on its microscopic understanding [1]. However, only a few integrable models can be solved rigorously [2]. Generally one has to rely on numerical simulations for non-integrable models. Thus it would be worthy to revisit the traditional kinetic approach by incorporating some microscopic consideration for the low dimensional non-integrable lattice systems.

According to the Debye formula, the thermal transport process in a nonlinear lattice is intrinsically relative to its dispersion relation and relaxation of normal modes (phonons). The existence of nonlinearity makes the definition of phonon delicate, and it is even harder in this case to quantify phonon transport from a first-principle way. To surmount the difficulties due to nonlinearity, the concept of “effective phonons” has been recently introduced to study heat conduction in dynamical models [3–6]. The basic idea consists in incorporating the nonlinearity into normal modes by renormalizing the harmonic frequency spectrum. In the serial studies [3–5], the authors apply the so-called effective phonon theory (EPT) to study heat conduction within the kinetic framework. In Ref. [6], the authors study heat conduction through a lattice consisting of two weakly coupled nonlinear segments via the self-consistent phonon theory (SCPT).

It is thus interesting to compare EPT and SCPT since they have both been applied to the field of heat conduction. In the present study, we will give a detailed comparison via the Debye formula as done in [3–5]. Our result shows the equivalence of SCPT and EPT in a large range of temperature. Considering the failure of the classical description at low temperature regime, we also compute quantum corrections to the thermal conductivity by extending our study to quantum regime, which gives qualitatively consistent results with

experimental studies.

It should be emphasized that both EPT and SCPT cannot give the microscopic definition of the relaxation time τ_k for phonons of mode k . A traditional perturbative way consists in studying the single mode relaxation time based on three- and four- phonon processes [7]. Great efforts have been devoted to obtain the relaxation time of the heat current correlations [8, 9], which in general might be related to the relaxation time of phonons. However, the relation was so far unclear. For an anharmonic chain, a simple but physically appealing assumption

$$\tau_k^{-1} \propto \omega_k \epsilon \quad (2)$$

has been proposed in Ref. [4], where ω_k is the phono frequency of mode k . The dimensionless nonlinearity ϵ is defined as the ratio between the average of the anharmonic potential energy and the total potential energy:

$$\epsilon = \frac{|\langle E_n \rangle|}{\langle E_l + E_n \rangle}. \quad (3)$$

One can see that, when ϵ vanishes, τ approaches to infinity, leading to the expected divergence of the thermal conductivity. In the following, we will apply the assumption of Eq. (2) to Eq. (1) in order to study the thermal conduction of an anharmonic chain, which gives surprising agreement with non-equilibrium simulations.

I. EFFECTIVE PHONON APPROACHES

In this section we will compare the SCPT (see, e.g., [10, 11]) and EPT [12, 13]. To make this concrete, we mainly focus on the temperature dependence of the physical quantities of the Fermi-Pasta-Ulam β (FPU- β) model, which is a classic example to study heat conduction. The Hamiltonian of the FPU- β model is given by

$$H = \sum \frac{p_i^2}{2} + \frac{K}{2}(x_{i+1} - x_i)^2 + \frac{\lambda}{4}(x_{i+1} - x_i)^4. \quad (4)$$

Within the SCP approximation, the Hamiltonian (4) is approximated by a trial Hamiltonian

$$H_0 = \sum \frac{p_i^2}{2} + \frac{f}{2}(x_{i+1} - x_i)^2, \quad (5)$$

where the effective harmonic coupling constant f is given by Eq. (A.29) in the appendix with the Boltzmann constant $k_B = 1$. Note that f is temperature dependent, which stems

from the existence of nonlinearity in the system. The dispersion relation of effective phonons corresponding to the effective Hamiltonian (5) can be written in the form

$$\omega_k = 2\sqrt{f} \sin \frac{k}{2}. \quad (6)$$

It is then straightforward to calculate the dimensionless nonlinearity ϵ and the specific heat C from gaussian averages of SCPT, which yields

$$\epsilon = \frac{f - K}{f + K}, \quad (7)$$

$$C = \frac{3}{4} + \frac{K}{4\sqrt{K^2 + 12\lambda T}}. \quad (8)$$

The derivation of the effective phonon spectrum is based on the generalized equipartition theorem,

$$k_B T = \left\langle q_k \frac{\partial H}{\partial q_k} \right\rangle_c, \quad (9)$$

where the bracket $\langle \cdot \rangle_c$ stands for a thermal average in the canonical ensemble and q_k denotes the Fourier transform of the coordinate x_i . The next step consists of an approximative transformation of the right hand side of Eq. (9) into a more compact form (see [3, 12] for details),

$$k_B T = \tilde{\omega}_k^2 \langle q_k^2 \rangle_c. \quad (10)$$

Specifically, the effective phonon spectrum $\tilde{\omega}_k$ for the FPU- β model reads as

$$\tilde{\omega}_k = 2\sqrt{\alpha} \sin \frac{k}{2}. \quad (11)$$

Here α is given by

$$\alpha = K + \lambda \frac{\langle \sum_i (x_{i+1} - x_i)^4 \rangle_c}{\langle \sum_i (x_{i+1} - x_i)^2 \rangle_c} = \frac{2\lambda T Y_{1/4}(x)}{K[Y_{3/4}(x) - Y_{1/4}(x)]}, \quad (12)$$

where $Y_{1/4}(x)$ and $Y_{3/4}(x)$ are the modified Bessel functions of the second kind and $x \equiv K^2/(8\lambda T)$. The parameters for the nonlinearity $\tilde{\epsilon}$ and the specific heat \tilde{C} that follow from EPT can be expressed in the form

$$\tilde{\epsilon} = \frac{K^2[Y_{1/4}(x) - Y_{3/4}(x)] + 2\lambda T Y_{1/4}(x)}{K^2[Y_{3/4}(x) - Y_{1/4}(x)] + 2\lambda T Y_{1/4}(x)}, \quad (13)$$

$$\tilde{C} = \frac{3}{4} + \frac{K^2}{16\lambda T} \frac{Y_{3/4}(x)}{Y_{1/4}(x)} + \frac{K^4}{64\lambda^2 T^2} \left(1 - \frac{Y_{3/4}(x)^2}{Y_{1/4}(x)^2}\right). \quad (14)$$

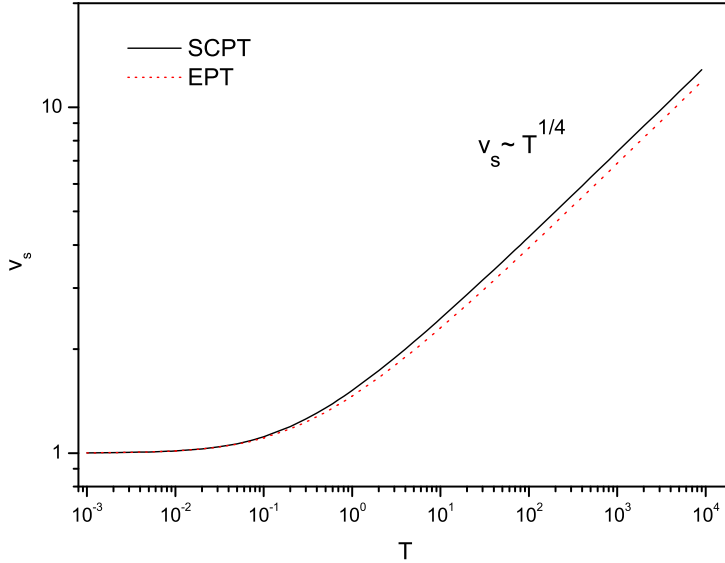


FIG. 1: Effective sound speed $v_s = \sqrt{f}$ as a function of temperature. At high temperature regime, $v_s \propto T^{1/4}$. Here $K = 1$, $\lambda = 1$.

In Fig. 1, we plot the effective sound speed $v_s \equiv \sqrt{f}$ (and $\tilde{v}_s \equiv \sqrt{\alpha}$) as a function of the temperature. The high temperature behavior gives $v_s \propto T^{1/4}$, which was already reported in Ref. [4, 14]. We also compare ϵ and C calculated from SCPT and EPT in Fig. 2 and Fig. 3, respectively. One can notice that SCPT and EPT yield practically the same temperature dependence over seven orders of magnitude.

We will now apply these two effective phonon approaches to calculate the thermal conductivity from the Debye formula (1). For the sake of simplicity, we will only present the derivation from SCPT. The phonon group velocity within SCPT is given by

$$v_k = \frac{\partial \omega_k}{\partial k} = \sqrt{f} \cos \frac{k}{2} \propto \sqrt{f}. \quad (15)$$

According to the assumption for the relaxation time (2), the mean free path reads as

$$l_k = v_k \tau_k \propto \epsilon^{-1}. \quad (16)$$

Substituting Eq. (15) and Eq. (16) into Eq. (1), the temperature dependence of the thermal conductivity can be given by [4]

$$\kappa(T) \propto \frac{C\sqrt{f}}{\epsilon}. \quad (17)$$

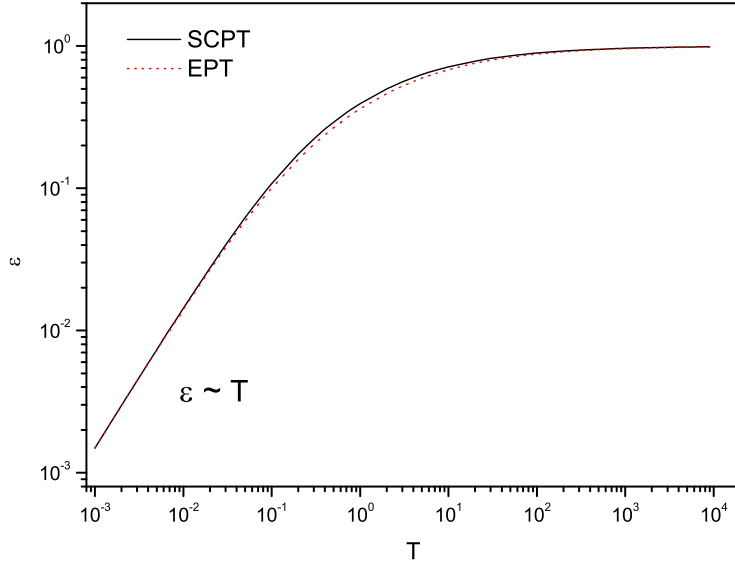


FIG. 2: Temperature dependence of the dimensionless nonlinearity ϵ . At low temperature regime $\epsilon \propto T$, while at high temperature limit $\epsilon \simeq 1$. Here $K = 1$, $\lambda = 1$.

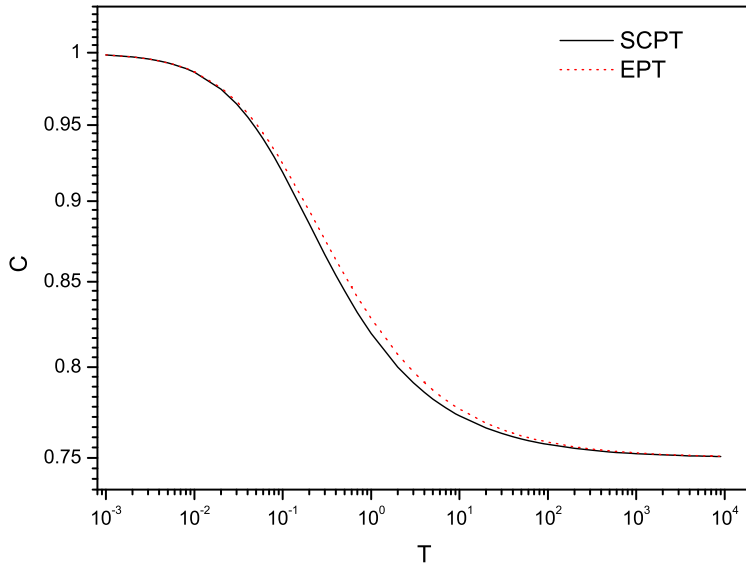


FIG. 3: Temperature dependence of specific heat. $C \simeq 1$ at low temperature regime (harmonic limit) and C approaches the lower limit $3/4$ at high temperature regime. Here $K = 1$, $\lambda = 1$.

The calculation of κ from EPT follows along similar lines. By replacing in Eq. (17) the specific heat, the group non-linearity and the non-linearity by their counterpart deduced from EPT, that is Eq. (12), (13) and (14), one obtains an alternative expression for the thermal conductivity (17). Note that we only consider the temperature dependence of κ here as in Ref. [4]. Nevertheless, it should be emphasized that κ is both temperature and size dependent. κ diverges in the thermodynamic limit due to the divergence of summation with respect to k in the acoustic regime, which is not the concern of this study.

The analytical prediction and the simulation result for the temperature dependence of κ are compared in Fig. 4 and Fig. 5 for $\lambda = 1$ and $\lambda = 0.1$, respectively. One can notice that the power law behavior observed in Ref. [4, 14], i.e., $\kappa \propto T^{-1}$ at low temperature regime and $\kappa \propto T^{1/4}$ at high temperature regime are exactly reproduced. As a comparison, non-equilibrium molecular dynamics simulations were performed by applying Langevin heat baths at the two ends of the chain [1]. In order to compute the thermal conductivity, a finite temperature difference with 10% deviation from the average temperature was consistently used. It is clearly seen that the analytical calculations, rescaled by a constant factor that is implicit in the Debye formula, give good agreements with the simulation results in a large range of temperature.

Both Fig. 4 and Fig. 5 show the existence of a minimum of κ at a specific temperature T_0 . By computing the derivative of the thermal conductivity with respect to T ,

$$\left. \frac{\partial \kappa}{\partial T} \right|_{T_0} = 0, \quad (18)$$

one easily obtains the turning point in the simple form

$$T_0 = g_0 \frac{K^2}{\lambda}. \quad (19)$$

Here we neglect the temperature dependence of the classical specific heat C , which has a very weak dependence on the temperature. The dimensionless constant g_0 is then given by

$$g_0 = \frac{7}{3} + \sqrt{5}, \quad (20)$$

If one takes into account the specific heat given by (8), the behavior of $T_0 \propto K^2/\lambda$ survives while g_0 should be replaced approximately by 5.52. The turning point T_0 denotes the transition of κ from decreasing behavior to increment behavior with increasing temperature.

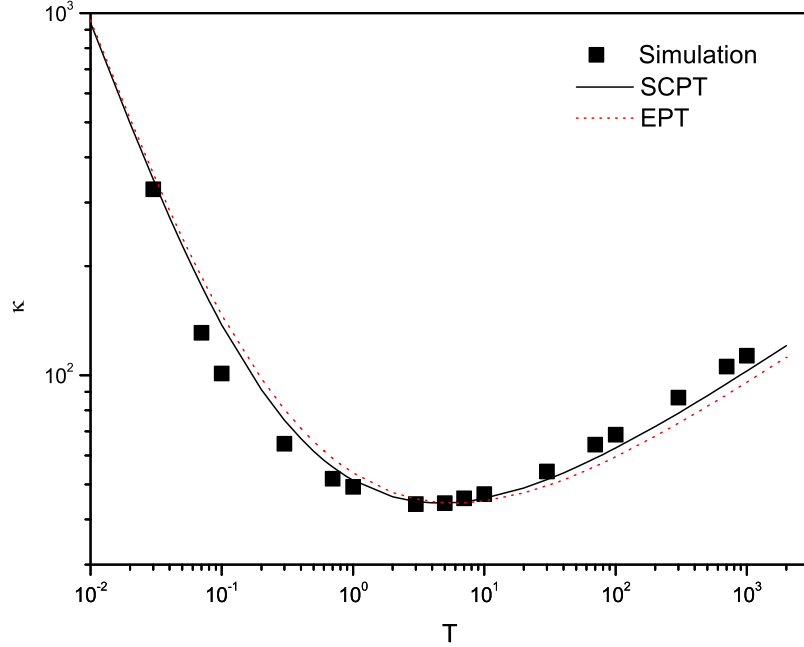


FIG. 4: Temperature dependence of thermal conductivity. Here $K = 1$, $\lambda = 1$, and system size $N = 1024$ for simulation. Analytical results (solid line and dot line) are rescaled (divided by a constant), which is consistent with simulation result in whole temperature range. The simulation result shows the temperature for the minimum of κ at $T_0 \approx 5$, in agreement with Eq. (19).

Eq. (19) can be understood by scaling the Hamiltonian (4) as done in Ref. [14]. Let

$$p_i = \frac{K}{\sqrt{\lambda}} \tilde{p}_i, \quad (21a)$$

$$x_i = \sqrt{\frac{K}{\lambda}} \tilde{x}_i, \quad (21b)$$

one obtains

$$H = \frac{K^2}{\lambda} \check{H}, \quad (22)$$

where the dimensionless Hamiltonian \check{H} reads as

$$\check{H} = \sum \frac{\tilde{p}_i^2}{2} + \frac{1}{2} (\tilde{x}_{i+1} - \tilde{x}_i)^2 + \frac{1}{4} (\tilde{x}_{i+1} - \tilde{x}_i)^4. \quad (23)$$

Eq. (21) leads to

$$T = \langle p_i^2 \rangle = \frac{K^2}{\lambda} \langle \tilde{p}_i^2 \rangle = \frac{K^2}{\lambda} \check{T}. \quad (24)$$

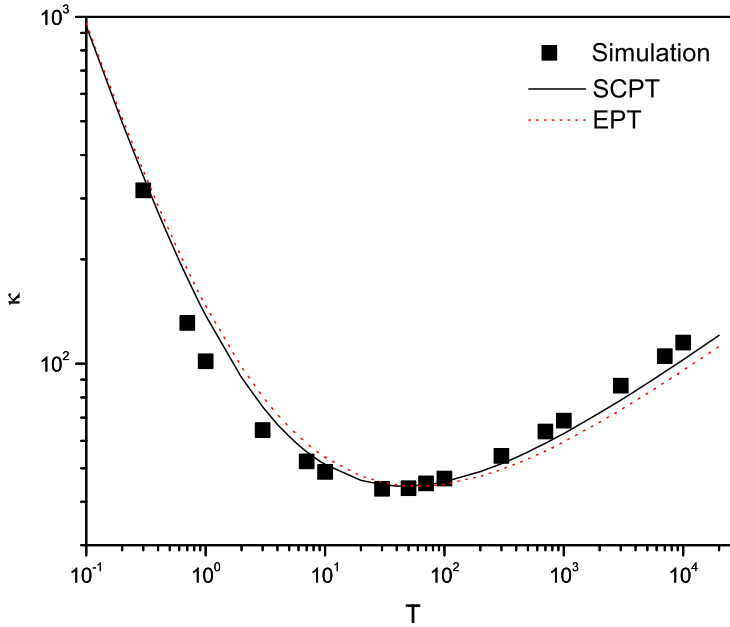


FIG. 5: Temperature dependence of thermal conductivity. Here $K = 1$, $\lambda = 0.1$, and $N = 1024$ for simulation. Like Fig. 4, analytical results are rescaled. The simulation result shows $T_0 \approx 50$, in agreement with Eq. (19).

Eq. (24) means that the temperature dependence of physical quantities of the FPU- β model can be rescaled according to the temperature transformation in Eq. (24), which can be verified in Fig. 6.

Note that the nonlinearity λ dependence of κ is similar with the temperature dependence shown in Fig. 4, Fig. 5 and Fig. 6. A critical nonlinearity λ_0 corresponding to the minimum of κ can also be similarly obtained as

$$\lambda_0 = g_0 \frac{K^2}{T}. \quad (25)$$

Eq. (19) and Eq. (25) shows that the temperature T and the nonlinearity λ are inversely equivalent.

Finally, it is interesting to note that

$$\epsilon(T_0) = \epsilon(\lambda_0) = \frac{\sqrt{5} - 1}{2}, \quad (26)$$

which is the well-known golden ratio. Due to the particular property of the golden ratio, the ratio of nonlinear potential and harmonic potential $\langle E_l \rangle / \langle E_n \rangle$ is also the golden ratio.

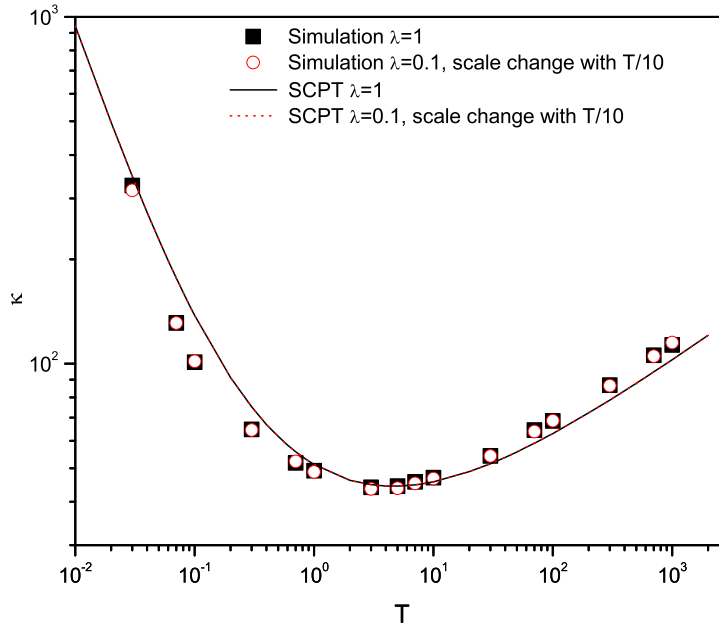


FIG. 6: Scaling of thermal conductivity. Here we simply apply coordinate transformation $\check{T} = T/10$ to Fig. 5 and then merge it with Fig. 4. One can see the overlap of the two figures, which indicates the scaling of thermal conductivity.

II. QUANTUM CORRECTIONS

From the experimental point of view, the thermal conductivity of real materials should vanish at zero temperature. This behaviour is inexistent within the classical description of heat conduction as shown above, since the latter leads to a divergent thermal conductivity at zero temperature. The disagreement between the classical description and experimental curves results from the inability of the classical physics to take into account the freezing of phonon modes, which is a pure quantum effect. We would like to emphasize that the consideration of the low temperature regime is not of pure theoretical interest. Generally, the Debye temperature of many solid systems is indeed well above ambient temperature. To name but a few, $T_D = 783$ K in stoichiometric CaB_6 and $T_D = 960$ K for vacancy doped EuB_6 [15]. In carbon nanotubes, the Debye temperature may even exceed 1000–2000 K [16]. One thus should take into account quantum effects, namely the partial thermalization of phonon modes even far above the room temperature for these materials.

In the following, we will treat the Debye equation for the FPU- β model semi-classically and show that the vanishing behaviour of κ manifests itself if one correctly takes into account the Bose-Einstein statistics. At this point, we should recall that the derivation of EPT is based on the classical equipartition theorem (see Eq. (9)). It is thus impossible to extent the effective phonon approach to the quantum regime, which makes SCPT more adequate since the latter can be derived from a purely quantum approach. The derivation of the quantum self-consistent phonon theory (QSCPT) is presented in the appendix. To avoid the divergence of Eq. (1) due to the goldstone mode ($k = 0$), a small quadratic on-site potential $f_0 x_i^2/2$ is included in the Hamiltonian (4). Here the constant f_0 is fixed to its lower-boundary ($f_0 = 10^{-6}$) so that its decrease below this limit doesn't change the value of κ . A strong point of QSCPT is that the approach unambiguously provides a mode decomposition for the specific heat and the phonon velocity, which allows one to consider in a rigorous way the discrete mode summation of the Debye equation (1). The specific heat per mode C_k is obtained from (A.24). The phonon velocity v_k follows from the derivative of the pseudo-phonon spectrum (A.21) and according to Eq. (16), the mean free path is given by $l_k = \tau_k v_k$ where $\tau_k^{-1} \propto \epsilon \omega_k$. For this model, the phonon frequency that should be numerically solved with Eq. (A.19) is

$$\omega_p^2 = f_0 + 4 \left(K + 3\lambda \langle \delta x^2 \rangle \right) \sin^2 \left(\frac{p\pi}{N} \right), \quad (27)$$

where the integer $p \in [1, N]$ and the phonon mode $k \equiv 2p\pi/N$. The non-linearity parameter is given by

$$\epsilon = \frac{\lambda \langle \delta x^4 \rangle / 4}{f_0 \langle x^2 \rangle / 2 + K \langle \delta x^2 \rangle / 2 + \lambda \langle \delta x^4 \rangle / 4}. \quad (28)$$

Fig. 7 gives the specific heat $C = 1/N \sum C_p$ as a function of the temperature. At the low temperature regime, C increases linearly with increasing temperature since the high energy modes are gradually thermalized. This is the well-known partial thermalization effect.

The agreement with the rigorous result for the harmonic chain ($\lambda = 0$) at low temperature regime shows that the harmonic quantum fluctuations play the dominant role. The quantum effect, as expected, is negligible above the Debye temperature $T_D = 2\sqrt{K} = 2$ and the system behaves like the classical one.

By collecting all the quantities in the Debye equation (1), we finally obtain the temperature dependence of the thermal conductivity from the quantum approach, which we compare

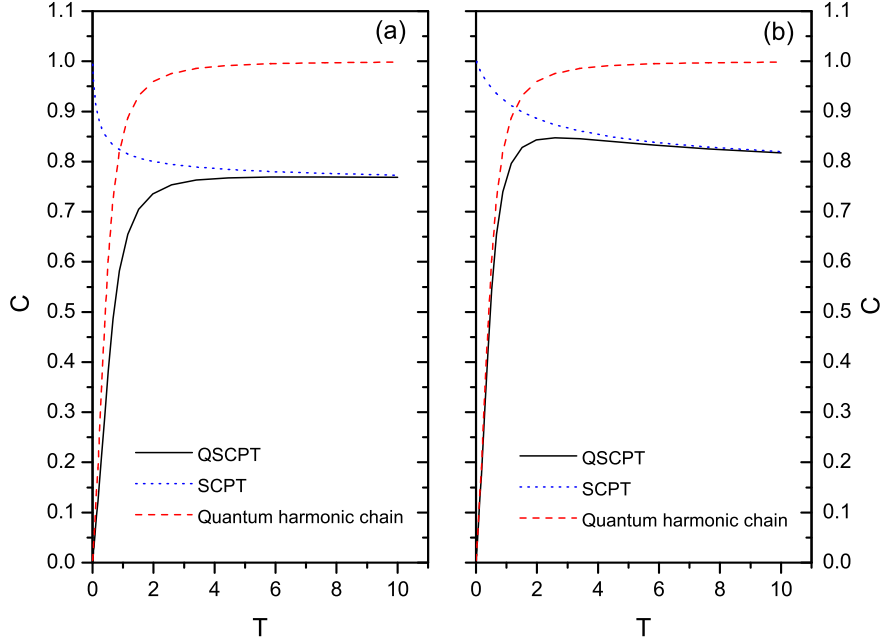


FIG. 7: Specific heat as a function of temperature for (a) $\lambda = 1$; (b) $\lambda = 0.1$. The harmonic potential is given by $V_0 = K\delta x^2/2 + f_0 x^2/2$. $K = 1$ and $f_0 = 10^{-7}$ for all cases. At low temperature regime, $C \propto T$.

in Fig. 8 with its classical counterpart. When the temperature is high enough, QSCPT reproduces the classical behavior as shown in Fig. 4 and Fig. 5, where the mean free path and the specific heat are nearly constant and the temperature dependence of κ mainly follows that of the sound speed $v_s \propto T^{1/4}$. The classical and quantum results agree up to the Debye temperature. The deviation of the quantum result takes place around T_D , which is followed by a peak at temperature $T_{max} \approx 1$, then the thermal conductivity drops to zero. T_{max} here indicates the lower bound of the temperature range over which *umklapp* processes [17] yield the dominant contribution to thermal conductivity. The existence of this peak results from a competition between the increasing behavior of the mean free path and the strongly decreasing tendency of the specific heat. The latter property is a consequence of the partial thermalization of high frequency phonons, which is a pure quantum effect explaining the failure of classical approaches below the Debye temperature. At low temperatures, the mean free path and the sound speed are nearly constant in the quantum case. The difference for the temperature dependence of κ is mainly due to the difference of the specific heat. Our

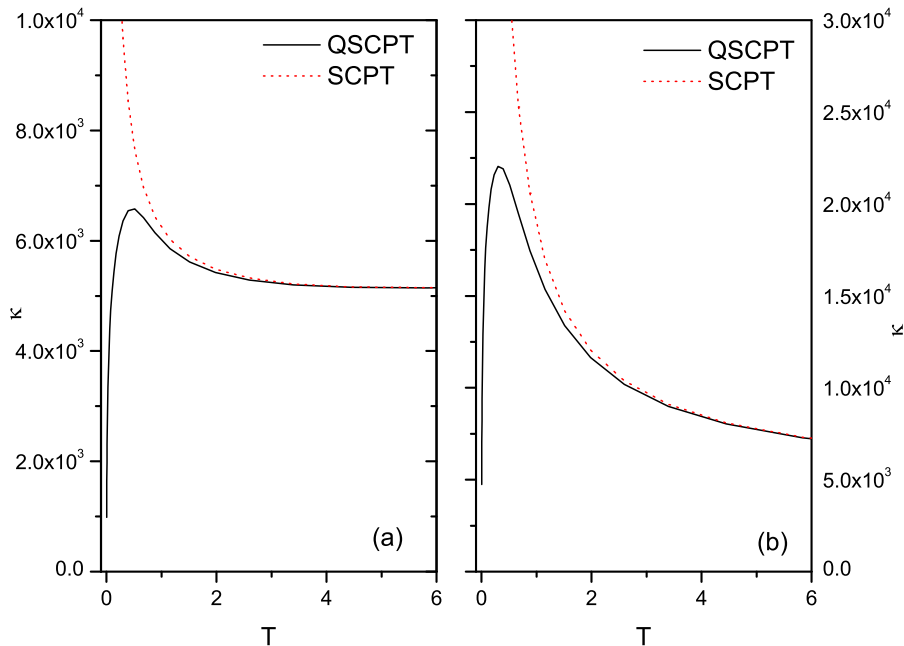


FIG. 8: Temperature dependence of thermal conductivity for (a) $\lambda = 1$; (b) $\lambda = 0.1$. $K = 1$ and $f_0 = 10^{-6}$ for both cases.

result based on QSCPT, characterized by the existence of the *umklapp* peak, is qualitatively consistent with the experimental studies (see, e.g., [16, 18–20]). Finally, one should note that the scaling behavior (24) is not applicable for quantum case.

III. SUMMARY

In summary, SCPT and EPT are compared in the present study. The basic difference between SCPT and EPT lies in the different way to calculate the statistical average of physical quantities. Specifically, the canonical average is applied in EPT but Gaussian average is applied in SCPT. We show that both SCPT and EPT give the same behavior for the thermodynamic quantities of a classical system, which indicates their equivalence. It seems that gaussian average is preferable for analytical derivation, especially for models with an on-site potential, since the thermal averages should be computed in this case from numerical transfer matrix calculations. The additional gain is that SCPT can be extended to study the quantum system, as shown in section II. Note that EPT is based on the assumption

of the equipartition theorem, whose validity in the quantum regime is broken. Thus QSCPT offers a simple way to explore for a given Hamiltonian model the low temperature physics related to the Bose-Einstein statistics.

We studied the temperature dependence of the thermal conductivity of the FPU- β model for both the classical and quantum case. The temperature for the minimum of $\kappa(T)$ was determined from the classical SCPT, which clearly shows the scaling behavior of thermal conductivity for this non-linear model. We also showed that non-equilibrium molecular dynamics simulations are in good agreement with the analytical results. At the low temperature regime, the semiclassical treatment of the Debye equation reproduced the *umklapp* peak, a well-known characteristic observed in experimental studies.

Acknowledgments

This work was supported in part by grants from the Hong Kong Research Grants Council (RGC) and the Hong Kong Baptist University.

Appendix: Quantum Self-Consistent Phonon Theory

In this appendix, we present a simple derivation of the first order self-consistent phonon theory for 1D Hamiltonian systems. The presented approach is similar to the derivation of the variational path integral method (see [21–23]). In the path integral representation of quantum statistical mechanics, the N -body partition function in the canonical ensemble can be expressed as a path integral over periodic trajectories, that is

$$Z = \int D\mathbf{x} e^{-S[\mathbf{x}]}, \quad (\text{A.1})$$

where

$$S = \int_0^{\hbar\beta} d\tau \left(\frac{m}{2} \dot{\mathbf{x}}^2 + U[\mathbf{x}] \right) \quad (\text{A.2})$$

is the Euclidean action and the first and second terms in the integral correspond to the total kinetic and potential energies. It is well known that an exact evaluation of the N -body path integral (A.1) for general anharmonic potentials is impossible. The idea of SCPT is basically approximating the original Euclidean action with a trial action that allows an exact evaluation of the trace (A.1). Since we deal in this work exclusively with 1D Hamiltonian

models with closest neighbor interactions of the form

$$H = \sum_{k=1}^N \left\{ \frac{m}{2} \dot{x}_k^2 + V(x_k) + W(\delta x_k) \right\}, \quad (\text{A.3})$$

where $\delta x_k = x_k - x_{k-1}$, an optimal choice of the trial Hamiltonian is that of a coupled harmonic oscillator chain,

$$H_0 = \sum_{k=1}^N \left\{ \frac{m}{2} \dot{x}_k^2 + \frac{\lambda_1}{2} x_k^2 + \lambda_2 x_k + g x_k x_{k-1} \right\}. \quad (\text{A.4})$$

The trial parameters λ_1 , λ_2 and g are to be deduced by minimizing the right hand-side of the Feynman-Jensen inequality,

$$\mathcal{F} \leq \mathcal{F}_0 + \langle H - H_0 \rangle, \quad (\text{A.5})$$

where $\mathcal{F}_0 = -k_B T \ln Z_0$. The trial partition function given by

$$Z_0 = \int D\mathbf{x} e^{-S_0[\mathbf{x}]/\hbar}, \quad (\text{A.6})$$

can be easily computed by first performing a Fourier decomposition of the periodic paths,

$$x_k = \sum_{n \geq 0} (x_{kn} e^{i\Omega_n t} + c.c.), \quad (\text{A.7})$$

where $\Omega_n = 2\pi n / (\beta\hbar)$ stand for Matsubara frequencies and the measure of integration of Eq. (A.6) has the form

$$D\mathbf{x} = \prod_{k,n} \frac{dx_{kn}^{re} dx_{kn}^{im}}{\sqrt{2\pi\beta\hbar^2/m}}. \quad (\text{A.8})$$

In the last expression as well as in Eq. (A.7), index k run over oscillators and n over Fourier components. We then substitute the expansion (A.7) into (A.4) and obtain the trial action by performing the integration over time τ ,

$$S_0 = \int_0^{\beta\hbar} d\tau H_0. \quad (\text{A.9})$$

The trial action S_0 that follows is a quadratic function of the Fourier components x_{kn} , that is

$$\begin{aligned} S_0 = & \beta\hbar \sum_{k=1}^N \left\{ \frac{\lambda_1}{2} x_{k0}^2 + \lambda_2 x_k + g x_{k0} x_{k-10} \right\} \\ & + \beta\hbar \sum_{k=1}^N \sum_{n \geq 1}^N \left\{ (\lambda_1 + m\Omega_n^2) \left(|x_{kn}^{re}|^2 + |x_{kn}^{im}|^2 \right) + 2g \left(x_{kn}^{re} x_{k-1n}^{re} + x_{kn}^{im} x_{k-1n}^{im} \right) \right\} \end{aligned} \quad (\text{A.10})$$

The next step consists of the trivial integration in Eq. (A.6) over Fourier components, which yields

$$Z_0 = \prod_{p=1}^N \frac{\sin(p\pi/N)}{\sinh(\beta\hbar\omega_p/2)}, \quad (\text{A.11})$$

for $\lambda_1 + 2g = 0$ and

$$Z_0 = e^{N\beta\frac{\lambda_1+2g}{2}\eta^2} \prod_{p=1}^N \frac{1}{2\sinh(\beta\hbar\omega_p/2)}, \quad (\text{A.12})$$

otherwise. In the last two expressions which give the zero-th order free energy \mathcal{F}_0 , we have defined the pseudo-phonon frequencies in the form

$$m\omega_p^2 = \lambda_1 + 2g - 4g \sin\left(\frac{p\pi}{N}\right) \quad (\text{A.13})$$

and an additional parameter

$$\eta = -\frac{\lambda_2}{\lambda_1 + 2g}. \quad (\text{A.14})$$

The calculation of the first order correction to free energy

$$\langle H - H_0 \rangle = \frac{1}{Z_0} \int D\mathbf{x} e^{-S[\mathbf{x}]} \left\{ \sum_{k=1}^N [V(x_k) + W(\delta x_k)] - H_0 \right\} \quad (\text{A.15})$$

proceeds in a similar way. The usual trick consists in expanding the on-site and inter-site potential in Fourier basis,

$$V(x_k) = \int \frac{dq}{2\pi} \tilde{V}(q) e^{iqx_k}, \quad W(\delta x_k) = \int \frac{dq}{2\pi} \tilde{W}(q) e^{iq\delta x_k}. \quad (\text{A.16})$$

Then we evaluate the average potentials per particle $\langle V(x_k) \rangle$ and $\langle W(\delta x_k) \rangle$ in (A.15) by integrating over Fourier components and finally invert the fourier transforms of Eq. (A.16). Consequently, the average value of the potential energies can be expressed in the form of smeared-out potentials,

$$V_\rho(\eta) \equiv \langle V(x_k) \rangle = \int \frac{dy}{\sqrt{2\pi\rho^2}} e^{-\frac{(y-\eta)^2}{2\rho^2}} V(y), \quad W_\gamma \equiv \langle W(\delta x_k) \rangle = \int \frac{dy}{\sqrt{2\pi\gamma^2}} e^{-\frac{y^2}{2\gamma^2}} W(y), \quad (\text{A.17})$$

where we have defined two parameters ρ^2 and γ^2 which correspond to lattice displacement and two-point correlation function, that is

$$\rho^2 \equiv \langle x_k^2 \rangle = \frac{\hbar}{2Nm} \sum_p \omega_p^{-1} \coth\left(\frac{\beta\hbar\omega_p}{2}\right) \quad (\text{A.18})$$

and

$$\gamma^2 \equiv \langle (x_k - x_{k-1})^2 \rangle = \frac{\hbar}{2Nm} \sum_p \frac{4 \sin^2 \left(\frac{p\pi}{N} \right)}{\omega_p} \coth \left(\frac{\beta \hbar \omega_p}{2} \right). \quad (\text{A.19})$$

The gaussian smearing (A.17) is a key characteristic of variational methods.

The first order free energy per particle can be finally expressed as

$$F_1 = F_0 - \sum_p \left\{ \frac{\beta \hbar \omega_p}{4} \coth \left(\frac{\beta \hbar \omega_p}{2} \right) \right\} + V_\rho(\eta) + W_\gamma. \quad (\text{A.20})$$

By minimizing this expression with respect to ω_p , one obtains the optimal pseudo-phonon frequency

$$\omega_p^2 = \frac{2}{m} \left\{ \frac{\partial V_\rho}{\partial \rho^2} + 4 \sin^2 \left(\frac{p\pi}{N} \right) \frac{\partial W_\gamma}{\partial \gamma^2} \right\}. \quad (\text{A.21})$$

On the other hand, the variation of Eq. (A.20) with respects to η yields

$$\frac{\partial V_\rho}{\partial \eta} = 0. \quad (\text{A.22})$$

Note that $\eta = 0$ for pair on site potentials ($V(x) = V(-x)$). Using (A.17), (A.18) and (A.21) in Eq. (A.20), we can further simplify the first order free energy in the form

$$F_1 = F_0 + V_\rho - \rho^2 \frac{\partial V_\rho}{\partial \rho^2} + W_\gamma - \gamma^2 \frac{\partial W_\gamma}{\partial \gamma^2}. \quad (\text{A.23})$$

The specific heat per mode can be then defined by

$$C_p = -T \frac{\partial^2 F_1}{\partial T^2}. \quad (\text{A.24})$$

One can easily obtain the classical limit of (A.23) by letting $\hbar \rightarrow 0$. The final result is

$$F_1 = \frac{1}{N\beta} \sum_p \ln(\beta \omega_p) + V_{\rho_c} - \rho_c^2 \frac{\partial V_{\rho_c}}{\partial \rho_c^2} + W_{\gamma_c} - \gamma_c^2 \frac{\partial W_{\gamma_c}}{\partial \gamma_c^2}, \quad (\text{A.25})$$

where ρ^2 and γ^2 in Eq. (A.23) are replaced by their classical counterpart,

$$\rho_c^2 \equiv \langle x_k^2 \rangle_{\hbar \rightarrow 0} = \frac{1}{Nm\beta} \sum_p \omega_p^{-2} \quad (\text{A.26})$$

and

$$\gamma_c^2 \equiv \langle (x_k - x_{k-1})^2 \rangle_{\hbar \rightarrow 0} = \frac{1}{Nm\beta} \sum_p \frac{4 \sin^2 \left(\frac{p\pi}{N} \right)}{\omega_p^2}. \quad (\text{A.27})$$

For FPU- β model (4),

$$W(\delta x_i) = \frac{K}{2} \delta x_i^2 + \frac{\lambda}{4} \delta x_i^4, \quad V = 0. \quad (\text{A.28})$$

Solving Eq. (A.27) self-consistently with Eq. (A.21), it is easy to get the effective harmonic constant

$$f = K + 3\lambda\gamma_c^2 = \frac{K + \sqrt{K^2 + 12\lambda K_B T}}{2}. \quad (\text{A.29})$$

-
- [1] S. Lepri, R. Livi, and A. Politi, *Phys. Rep.* **377**, 1 (2003).
 - [2] Z. Rieder, J. L. Lebowitz, and E. Lieb, *J. Math. Phys.* **8**, 1073 (1967).
 - [3] N. Li, P. Tong, and B. Li, *Europhys. Lett.* **75**, 49 (2006).
 - [4] N. Li and B. Li, *Europhys. Lett.* **78**, 34001 (2007).
 - [5] N. Li and B. Li, *Phys. Rev. E* **76**, 011108 (2007).
 - [6] B. Hu, D. He, L. Yang, and Y. Zhang, *Phys. Rev. E* **74**, 060101(R) (2006).
 - [7] G. P. Srivastava, *The Physics of Phonons* (IOP Publishing Ltd, Bristol, 1990).
 - [8] S. Lepri, *Phys. Rev. E* **58**, 7165 (1998).
 - [9] S. Lepri, R. Livi, and A. Politi, *Europhys. Lett.* **43**, 271 (1998).
 - [10] P. Brüesch, *Phonons: Theory and Experiments I*, Lattice Dynamics and Models of Interatomic Forces (Springer-Verlag, New York, 1982).
 - [11] T. Dauxois, M. Peyrard, and A. R. Bishop, *Phys. Rev. E* **47**, 684 (1993).
 - [12] C. Alabiso, M. Casartelli, and P. Marenzoni, *J. Stat. Phys.* **79**, 451 (1995).
 - [13] C. Alabiso and M. Casartelli, *J. Phys. A* **34**, 1223 (2001).
 - [14] K. Aoki and D. Kusnezov, *Phys. Rev. Lett.* **86**, 4029 (2001).
 - [15] K. Giannò, A. V. Sologubenko, H. R. Ott, A. D. Bianchi, and Z. Fisk, *J. Phys.: Condens. Matter* **15**, 6739 (2003).
 - [16] D. G. Cahill, W. K. Ford, K. E. Goodson, G. D. Mahan, A. Majumdar, H. J. Maris, R. Merlin, and S. R. Phillpot, *J. Appl. Phys.* **93**, 793 (2003).
 - [17] R. E. Peierls, *Quantum Theory of Solids* (Oxford University Press, London, 1955).
 - [18] J. Hone, M. Whitney, C. Piskoti, and A. Zettl, *Phys. Rev. B* **59**, R2514 (1999).
 - [19] M. S. Dresselhaus and P. C. Eklund, *Adv. Phys.* **49**, 705 (2000).
 - [20] D. G. Cahill, K. Goodson, and A. Majumdar, *J. Heat Transfer* **124**, 223 (2002).
 - [21] R. P. Feynman and H. Kleinert, *Phys. Rev. A* **34**, 5080 (1986).
 - [22] H. Kleinert, *Path Integrals in Quantum Mechanics, Statistics, and Polymer Physics* (World

Scientific, Singapore, 1995), 2nd ed.

- [23] R. Giachetti and V. Tognetti, Phys. Rev. B **33**, 7647 (1986).